1 Introduction

During the SARS-COV-2 pandemic, epidemic models were shown to fail in accounting for human behavior and the heterogeneous structure of the contact network, both of which significantly impact epidemic dynamics [**?**]. Non-pharmaceutical interventions such as travel restrictions have proven essential in preventing the spread of the virus. However, the efficiency and restraint in implementing such restrictions must consider economic costs and potential societal backlash due to prolonged quarantine periods.

Epidemic models started with focusing on just a single homogeneously mixed population, which was known to be a severe simplification of the typically heterogeneously structured contact patterns of social networks. To account for this, extensions of epidemic models have been made by applying them to complex networks, which take into account the irregular degree distribution of most social networks. Recently, a more hybrid model has been explored, termed metapopulation network, where a network of subpopulations have a network topology connecting them. Individuals in a subpopulation interact homogeneously with each other and migrate along the links to neighboring subpopulations with a mobility rate. Such a network is called a reaction-diffusion metapopulation network. This model is especially useful in systems that have sufficient network modularity where it can be accurately represented as a group of exclusive communities. Such examples of this are districts, cities, or even countries.

In this study, we introduce an extension to the existing model by incorporating adaptive mobility in the network. Subpopulations can restrict the mobility of incoming and outgoing individuals based on the prevalence of infections in incoming individuals from neighboring subpopulations.

List of Symbols

Symbol	Description
S_x, I_x, R_x	Susceptible, Infected, and Recovered individuals in subpopulation x
β	Infection rate in subpopulation x
γ	Recovery rate in subpopulation x
$\mathcal{X}$	Set of all subpopulations
μ	Mobility rate scalar between subpopulations
$\rho_{x,x'}$	Travel restriction scalar values for individuals traveling from subpopulation x to x'
$\bar{\rho}_{x,x'}$	Complementary of travel restriction, $\bar{\rho}_{x,x'} = 1 - \rho_{x,x'}$
t_x	Point in time in which $I_x(t) = i_0$
Δt_x	The delay in time between t_x and t'_x where x' is the upstream subpopulation
$W(x)$	The Lambert W function; solution of $y\ e^y = z$
F_2	Final cumulative infected flow from subpopulation 1 to subpopulation 2
t_{f2}	Time at which $I_2(t) \approx F_2$
λ	Control parameter for travel restriction rate of change
i_0	Initial condition for infected individuals in subpopulation 1
κ	Effective growth rate coefficient of an infected population as a proportion of its current infected individuals in 1-lattice graph ($\kappa = \beta - \gamma - 2\mu$)
c	Dimensionless constant $c = i_0\mu\lambda/\kappa$

Analysis

Let the network have a path graph (1-lattice graph) where subpopulation 1 is at the start of the path and has an initial infection of $I_1(0) = I_0$. The governing dynamics of the infection in subpopulation 1 is:

$$\dot{I}_1(t) = (\beta S_1 - \gamma)I_1 + \mu I_2 - 2\mu I_1$$

Since I_2 starts at zero and the susceptible fraction starts at one, a first-order approximation can be made:

$$\dot{I}_1 \approx (\beta - \gamma - 2\mu)I_1$$

For a randomly selected subpopulation j, the infection fraction dynamics can be represented and approximated as:

$$\dot{I}_j = (\beta S_j - \gamma)I_j + \mu(I_{j-1} + I_{j+1} - 2\mu I_j)$$

Since the diffusion of infected individuals starts from index 1 and increasing, $I_{j+1} \approx 0$ with respect to I_j. Similar to the above linearization:

$$\dot{I}_j \approx \kappa I_j + \mu I_{j-1}$$

where $\kappa = \beta - \gamma - 2\mu$. Solving the differential equation for the linearized $\dot{I}_1$:

$$I_1 = I_0 e^{\kappa t}$$

Substituting for $j = 2$ in the equation above:

$$\dot{I}_2 = \kappa I_j + \mu I_0 e^{\kappa t}$$

This ODE can be solved analytically which results in:

$$I_2 = I_0 \mu t e^{\kappa t}$$

Consequently, for $\dot{I}_3$:

$$\dot{I}_3 = \kappa I_j + \mu^2 \kappa t e^{\kappa t}$$

$$I_3 = I_0 \frac{\mu^2 t^2}{2} e^{\kappa t}$$

Through induction, it can be found that:

$$I_j = I_0 \frac{\mu^{j-1} t^{j-1}}{(j-1)!} e^{\kappa t}$$

To find the spread rate of the infection across the network, we solve for the time $t_{I_{j+1}=I_0} := t_j$:

$$I_0 \frac{\mu^j t_j^j}{j!} e^{\kappa t_j} = I_0$$

$$\frac{\mu^j t_j^j}{j!} e^{\kappa t_j} = 1$$

This unfortunately does not have a closed-form solution. However, a unique solution is guaranteed to exist, and since the function is monotonic and the root is simple, the solution can be found very easily numerically. To alleviate the numerical instability of higher and higher powers and factorial values, the log transform of the equation is solved instead:

$$\kappa t_j + j \ln(\mu t_j) - \ln(j!) = 0$$

where the log of the factorial has very stable methods to solve[**?**].

To test this solution, the expected time for $I_j = I_0$ was found numerically through simulation of the ODEs for a path graph network and also computed numerically from equation (7).

It was found that equation (6) was remarkably accurate in estimating the spread infection day of the subpopulations. Furthermore, the peak infection day can be inferred from the spread infection day as they each converge to the same slope, and the offset between them is approximately the time taken for one subpopulation to reach the peak infection day starting from I_0.

Since we are interested in the spread rate of the infection, the objective is to derive the value $\Delta t_{j+1} := t_{j+1} - t_j$. To do so, we first use equation (7) to find t_{j+1}:

$$\kappa t_{j+1} + (j+1) \ln(\mu t_{j+1}) - \ln((j+1)!) = 0$$

Based on numerical results, we found that Δt_j converges quickly to a constant value. Therefore, we apply an ansatz $\Delta t_{j+1} = t_{j+1} - t_j \approx \Delta t$ for $j \gg 1$, leading to $t_j \approx j\,\Delta t$.

Subtracting equation (7) from equation (8), we get:

$$\kappa \Delta t + j \ln\left(\frac{t_{j+1}}{t_j}\right) + \ln\left(\frac{\mu t_{j+1}}{j+1}\right) = 0$$

After substituting $t_j \approx j\,\Delta t$, we find:

$$\kappa \Delta t + j \ln\left(\frac{j+1}{j}\right) + \ln(\mu \Delta t) = 0$$

Taking $\lim_{j\to\infty}$, and using $\ln\left(\frac{j+1}{j}\right) \approx \frac{1}{j}$, we get:

$$\kappa \Delta t + \ln(\mu \Delta t) + 1 = 0$$

This is still a transcendental function. However, a known solution for this equation uses the Lambert W function. Applying it here results in:

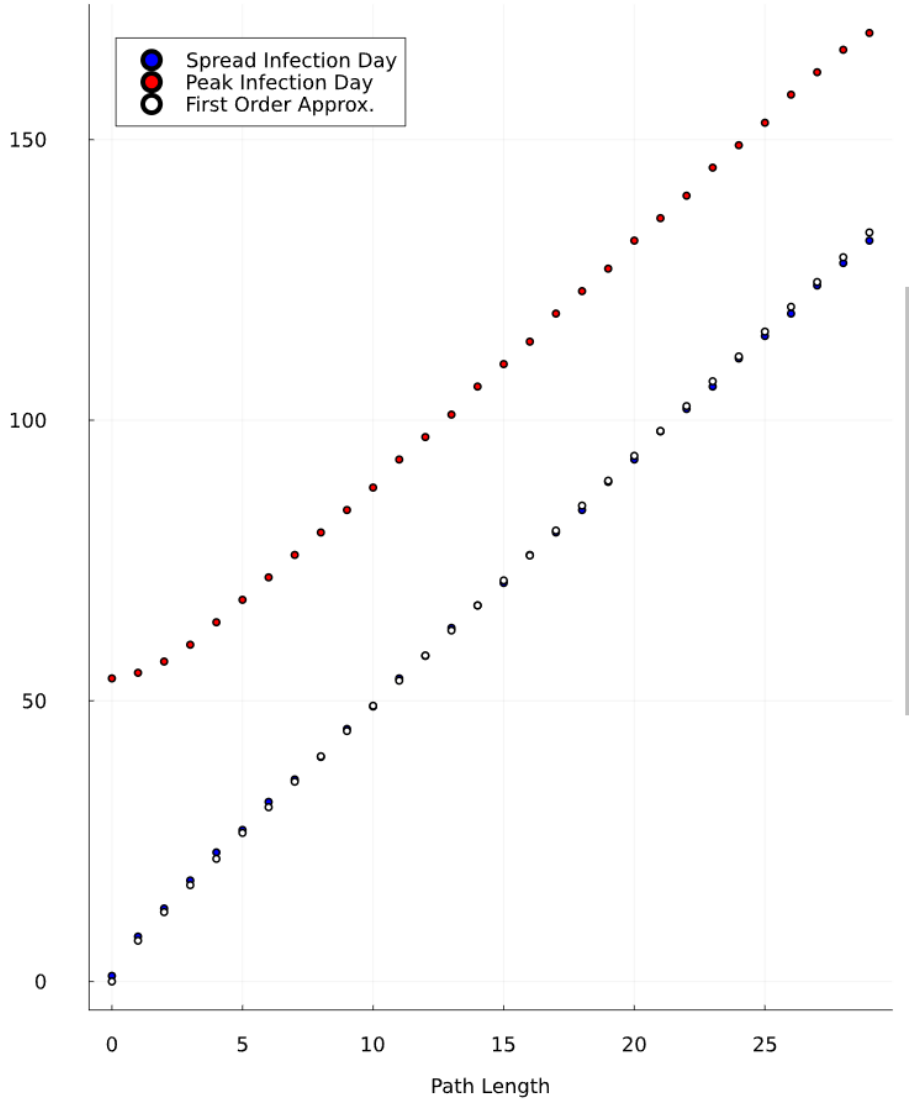

Figure 1: Simulation vs. analytical results for infection spread day. It can be seen that the time between $I_x(t) = i_0$ and $I_x(t) = sup(I_x(t))$ converges to a constant delay. Though this relationship, the spread infection days can be used to find the peak infection days.

$$\Delta t = \frac{1}{\kappa} W\left(\frac{\kappa}{e\mu}\right)$$

The next step is to derive the impact of the reactivity constant λ on the spread rate and extrapolate this spread rate on more complex network topologies such as small-world networks and scale-free networks.

We again evaluate the same system but with individual restriction adaptivity, where $\bar{\rho} := 1 - \rho$ and $\rho(0) = 0$:

$$\dot{\rho}_{x,x'} = \lambda\mu\bar{\rho}(I_{x'} - I_x)$$
$$\dot{I}_x = \beta SI - \gamma I + \sum_{x'} \mu(I_{x'} - I_x)\bar{\rho}_{x,x'}$$

We also define the flow $f_{x,x'}(t)$, which is the rate of incoming infected individuals per unit time from subpopulation x into x', where

$$f_{x,x'}(t) = \mu \bar{\rho}_{x,x'} I_{x'}$$

Applying the same linearization as equation (4):

$$\dot{I}_j \approx \kappa I_j + \mu \bar{\rho} I_{j-1}$$

Substituting $I_1 = i_0 \kappa e^{\kappa t}$ in equation (13):

$$\dot{\bar{\rho}}_2(t) = -i_0 \lambda \mu \bar{\rho}_2(t) e^{\kappa t}$$

The ODE in equation (13) can be solved using separation of variables as follows:

$$\dot{\bar{\rho}}_2(t) = -i_0 \lambda \mu \bar{\rho}_2(t) e^{\kappa t}$$

With the initial condition $\bar{\rho}_2(0) = 1$, we proceed as follows: Dividing both sides by $\bar{\rho}_2$ and multiplying by dt, then integrating both sides:

$$\int \frac{1}{\bar{\rho}_2} \, d\bar{\rho}_2 = -i_0 \lambda \mu \int e^{\kappa t} \, dt$$

$$\ln \bar{\rho}_2(t) = -\frac{i_0 \lambda \mu}{\kappa} e^{\kappa t} + C_1$$

Exponentiating both sides:

$$\bar{\rho}_2(t) = e^{C_1} e^{-\frac{i_0 \lambda \mu}{\kappa} e^{\kappa t}}.$$

Using $\bar{\rho}_2(0) = 1$ to find C_1:

$$\bar{\rho}_2(t) = e^{\frac{i_0 \lambda \mu}{\kappa}} e^{-\frac{i_0 \lambda \mu}{\kappa} e^{\kappa t}} = \exp\left(\frac{i_0 \lambda \mu}{\kappa} \left(1 - e^{\kappa t}\right) \right)$$

where $c := i_0 \lambda \mu / \kappa$ is a dimensionless constant.

This shows that the rate of decay for the first applied restriction based on this adaptive strategy is super-exponential. This is an intuitive outcome of having the rate of change of ρ be proportional to the incoming infected, which itself grows exponentially due to the internal infection rate. When simulating this system with sufficiently large λ, a somewhat unexpected result appears: it is found that adaptivity only delays the global infection spread instead of slowing down the spread rate. This can be seen in the infected evolution in all nodes in a simple SI epidemic model.

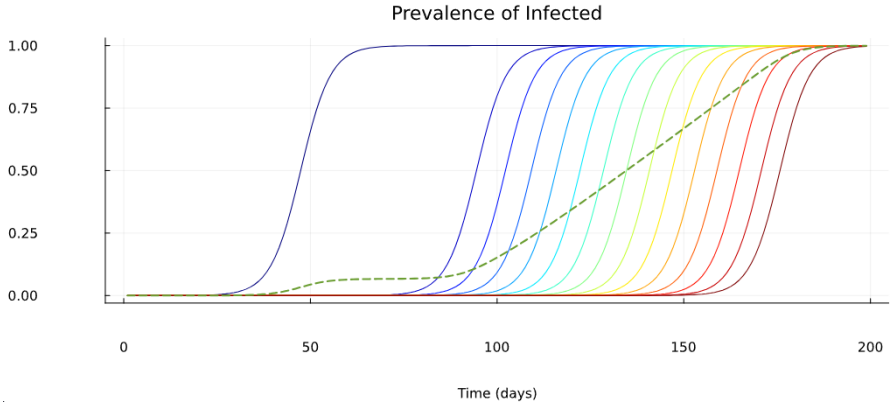

Figure 2: Evolution of infected population in an adaptive SI model on a 1-lattice graph (path graph) with $\lambda = 1e10$ and $i_0 = 1e-5$. It can be seen that there is a significant delay between the infection in the first subpopulation (the one with an initial infected prevalence i_0, and the rest of the metapopulation. The spread rate among the rest of the network is the same as with no adaptivity.

It is also worth noting that due to this super-exponential growth, $\rho_{2,1}$ decays down to zero much faster than the internal infection spread I_2. This difference in rates can be used to analytically

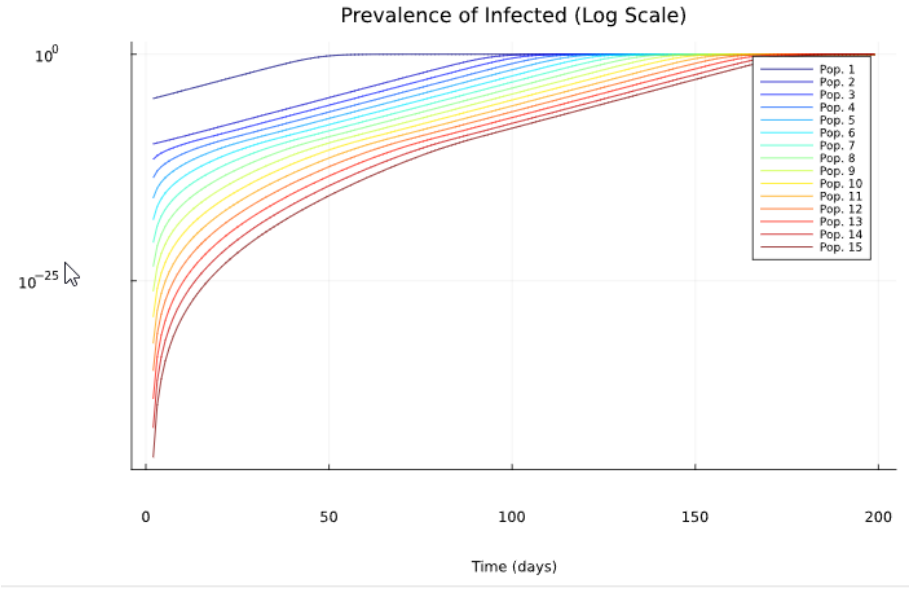

Figure 3: The same plot of the infected evolution in log-y scale. Zero-values of infection have been omitted from this plot, all of which exist at day 1. This scale helps show that the first subpopulation starts at an initial infected prevalence of $i_0 = 1e-5$ and the grows exponentially, which can be seen by the constant-slope line of the evolution with a slope $1/\kappa$. This same exponential evolution can also be seen for subpopulation 2, quickly reaches the value of F_2 when $\rho_{2,1}$ reaches 1. A later figure will show the growth towards this value. Interestingly, the remainder of the subpopulations have a non-linear slope until it reaches the same threshold F_2 at which point their respective restriction completely shut down and their behavior turns purely exponential

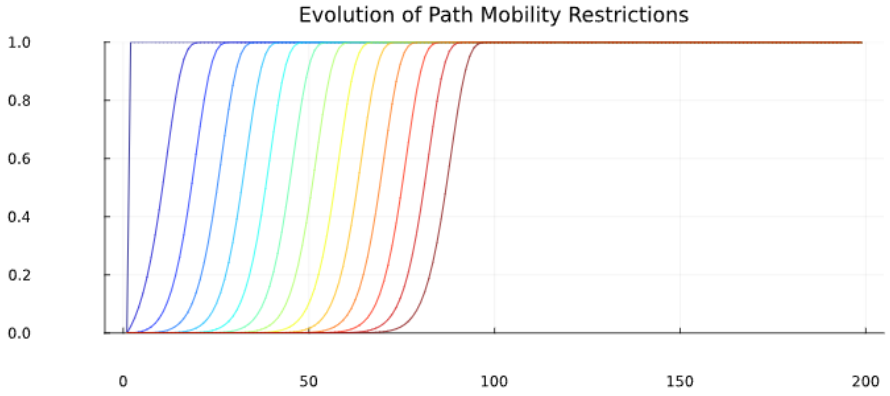

Figure 4: Evolution of mobility restrictions. It is worthy of note here that most ρ values reach 1 significantly before the populaiton's corresponsponding infected prevalence reaches any significant value. It can be also seen from this plot that ρ_2 reaches 1 before the second day of the scenario, while rho_3 has a non-zero initial growth rate.

approximate the delay in infection spread t_2 in subpopulation 2 from subpopulation 1. This can be done by first finding the final cumulative amount of incoming infecteds F_2 where

$$F_2 := \int_0^\infty f_2(t)dt$$

where

$$f_2(t) = \mu\bar{\rho}_2(t)I_1(t) = \mu \exp\left(c\left(1-e^{\kappa t}\right)\right) i_0 e^{\kappa t} = \mu i_0 \exp\left(c\left(1-e^{\kappa t}\right)+\kappa t\right)$$

An analytic solution for F could be found using the exponential integral Ei function $\int \exp(\exp(x))\,dx = \int \frac{\exp(u)}{u}\,du = \mathrm{Ei}(u) = \mathrm{Ei}(\exp(x))$. However, a linearization of the exponent term was found to be sufficiently accurate based on the numerical simulation. We define the expression $E(t) := c\left(1 - e^{\kappa t}\right) + \kappa t$ and linearize it around $t = 0$:

$$E(t) \approx (-c\kappa + \kappa)t = \kappa(1 - c)t$$

substituting the linearized $E(t)$ and $f_2(t)$ back into F_2, we get:

$$F_2 = \int_0^\infty \mu i_0 \exp\left(\kappa(1 - c)t\right) dt = \frac{\mu i_0}{\kappa(c - 1)}$$

dividing the numerator and denominator by $c = \frac{i_0 \lambda \mu}{\kappa}$:

$$F_2 = \frac{\frac{\kappa}{\lambda}}{\kappa\left(1 - \frac{1}{c}\right)} = \frac{1}{\lambda\left(1 - \frac{1}{c}\right)} \tag{1}$$

While F_2 is evaluated from $t = 0$ to ∞, due to the super-exponential rate of f_2, $F_2 = F_2(\infty) \approx F_2(t_{f2})$ where t_{f2} is a point in time where $\bar{\rho}(t_{f2}) \approx 0$ $I(t_{f2}) \approx F_2$. This approximation can be validated by checking the value of I_2 in the numerical solution of the ODE at the point in time where $\bar{\rho}(t) \approx 0$ and check if $I(t) \approx F_2$.

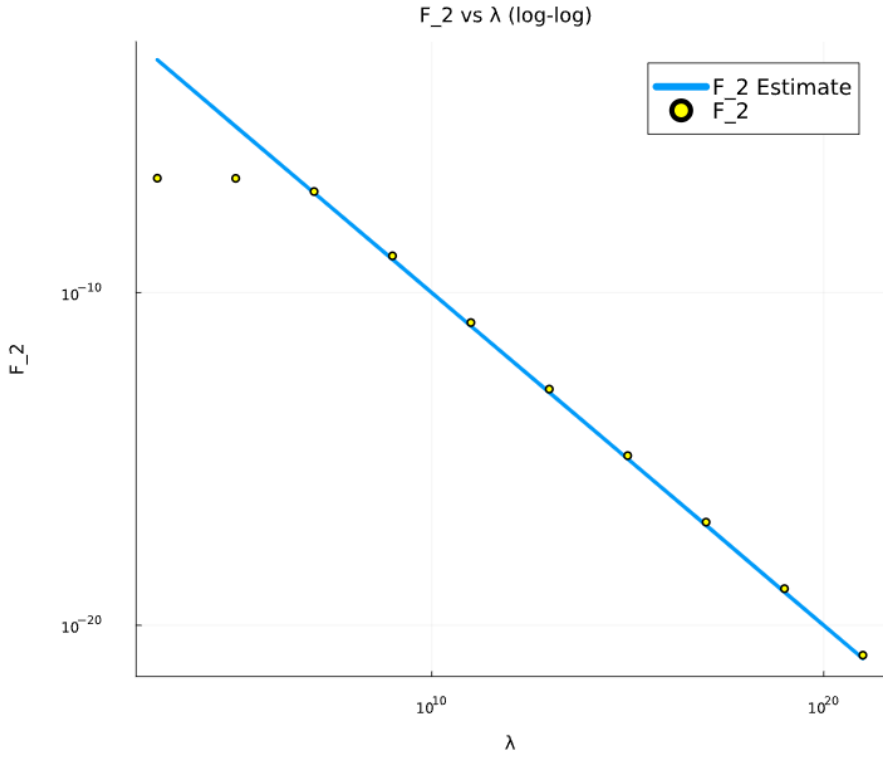

Figure 5: Validation of I_2 approximation at $t \approx t_{f2}$. The F_2 Estimate is $1/\lambda$ which in a log-log scale has a slope of -1. As can be seen here, this approximation is only valid for $\lambda > 1/i_0$. Before this threshold, there is approximately no dependency of F_2 on λ

This observation allows us to solve a simplified version of the ODE $\dot{I}_2(t)$ starting from $t = t_f$, with the initial conditions at that point in time.

$$I_2(t) = \int_{t_{f2}}^{t} \left(i_0 \mu \bar{\rho}_2(t) e^{\kappa t} + \kappa I_2(t)\right) dt$$

since $\bar{\rho} \approx 0$ for $t \geq t_{f2}$

$$I_2(t) = \int_{t_{f2}}^{t} \kappa I_2(t)dt = I_2(t_{f_2})e^{\kappa t} = F_2 e^{\kappa t} = \frac{e^{\kappa t}}{\lambda}$$

to find t_2, the value at which $I_2(t) = i_0$,

$$I_2(t) = \frac{e^{\kappa t_2}}{\lambda} = i_0$$

solving for t_2:

$$t_2 = \frac{\ln(i_0 \lambda)}{\kappa}$$

This relationship, as with the one for F_2, is only valid for $\lambda > \frac{1}{i_0}$. The most important observation from this finding is that the delay in infection depends on the logarithm of λ, which means there is very diminishing returns to increasing the adaptivity rates of travel restriction to infection. To validate this finding, t_2 was evaluated for different systems of ODEs with varying values of λ and κ:

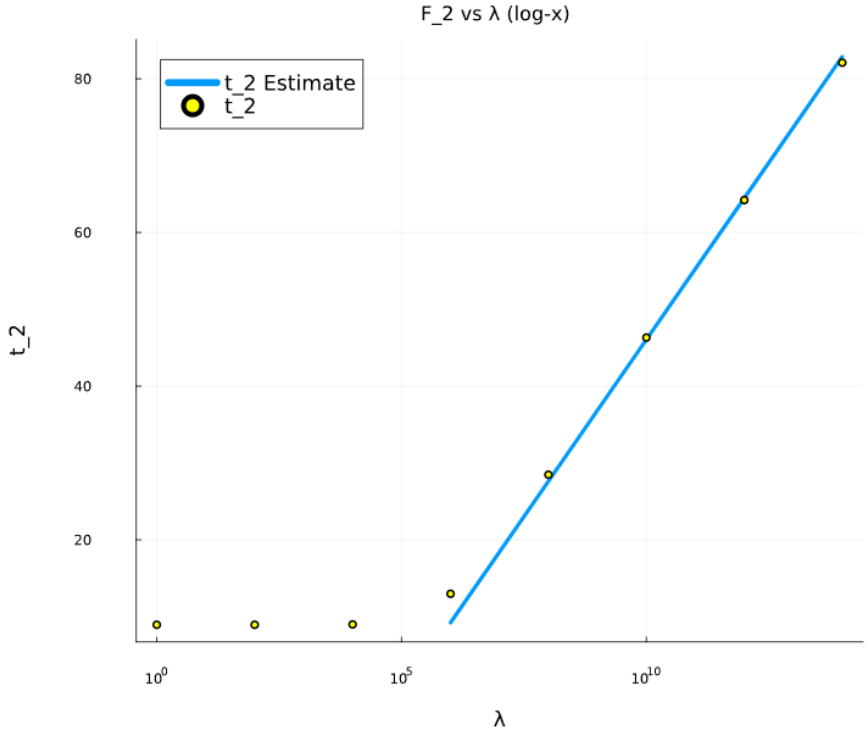

Figure 6: Evaluation of t_2 for different λ and κ values with the t_2 approximation in a log-x scale. The straight line in this plot correponds to a logarithmic dependency of t_2 on λ, as was found in the analytical approximation. The approximation is only valid for $\lambda > i_0$, which is 10^5 in this case. It can be seen that before this threshold, the impact of λ is negligible and t_2 has the same value as if there was no adaptivity.

It can proven that, for a sufficiently large λ, $I_3(t_{F2}) = \mu/\lambda$. (I just need to write it out and validate it numerically for different combination of μ and λ.

$$\dot{I}_2(t < t_{F2}) = f_2 = \mu i_0 e^{\kappa(1-c)t} \approx \mu i_0 e^{-\kappa c t}$$

$$I_2(t < t_{F2}) = \mu i_0 \left(\frac{e^{-\kappa c t}}{-\kappa c} - \frac{1}{-\kappa c} \right) = \frac{\mu i_0}{\kappa c} \left(1 - e^{-\kappa c t}\right) = \frac{1}{\lambda} \left(1 - e^{-\kappa c t}\right)$$

$$\dot{\bar{\rho}}_3 = -\lambda\mu\bar{\rho}_3\frac{1}{\lambda}\left(1-e^{-\kappa ct}\right) = -\mu\bar{\rho}_3\left(1-e^{-\kappa ct}\right)$$

$$\int\frac{d\bar{\rho}_3}{\bar{\rho}_3} = \int\mu(e^{-\kappa ct}-1)$$

$$\ln|\bar{\rho}_3| = \frac{-\mu e^{-\kappa ct}}{\kappa c} - \mu t + C_2$$

$$\bar{\rho}_3(t<t_{F2}) = \exp\left(\frac{1}{\lambda i_0} - \frac{e^{-\kappa ct}}{\lambda i_0} - \mu t\right)$$

$$f_3(t) = \mu\bar{\rho}_3(t)I_2(t) = \mu\exp\left(\frac{1}{\lambda i_0} - \frac{e^{-\kappa ct}}{\lambda i_0} - \mu t\right)\frac{1}{\lambda}\left(1-e^{-\kappa ct}\right)$$

$$f_3(t) = \frac{\mu}{\lambda}\left(\exp\left(\frac{1}{\lambda i_0} - \frac{e^{-\kappa ct}}{\lambda i_0} - \mu t\right) - \exp\left(\frac{1}{\lambda i_0} - \frac{e^{-\kappa ct}}{\lambda i_0} - \mu t - \kappa ct\right)\right)$$

$$f_3(t) \doteq \frac{\mu}{\lambda}\left(\exp\left(-\frac{-\kappa ct}{\lambda i_0} - \mu t\right) - \exp\left(-\frac{-\kappa ct}{\lambda i_0} - \mu t - \kappa ct\right)\right) = \frac{\mu}{\lambda}\left(1-\exp\left(-\kappa ct\right)\right)$$

$$F_3(t) = \int_0^\infty f_3(t) = \frac{\mu}{\lambda}$$

2 Model

To model the epidemic dynamics within each subpopulation, we use a mean-field compartmental model, assuming homogeneous mixing of individuals. Specifically, we employ the SIR model (Susceptible, Infected, and Recovered/Removed), which is commonly used as a simple epidemic model. The model follows a deterministic Poisson process where individuals can transition between compartments based on predefined rules. In the SIR model, the transition rules are: $S + I \to 2I$ (an infected individual infects a susceptible individual) and $I \to R$ (an infected individual recovers). No immunization loss process is considered in this model, focusing on a single-wave scenario. The model for each subpopulation x is described by the following set of ordinary differential equations (ODEs):

$$\begin{aligned}\dot{S}_x &= -\beta_x S_x I_x,\\ \dot{I}_x &= \beta_x S_x I_x - \gamma_x I_x,\\ \dot{R}_x &= \gamma_x I_x,\end{aligned}$$

where β_x and γ_x represent the infection and recovery rates at site x, respectively. The term $S_x I_x$ approximates the interaction rate between susceptible and infected individuals, which is valid for large populations. The transition rates are assumed to be uniform across all subpopulations, and each subpopulation has a total number of individuals $N_x = S_x + I_x + R_x$.

A simplified mechanistic approach is used, assuming a Markovian process in which the movement of individuals between subpopulations is governed by a matrix Δ, where Δ_{ij} represents the rate at which individuals move from subpopulation i to subpopulation j per unit time. Although a unique Δ matrix could be defined for each state (S, I, or R), for simplicity, we unify the mobility for all states. The most general model is described by the following system of ODEs:

$$\begin{cases}\dot{S}_x = -\beta_x S_x I_x - \mu_{(S)} \sum_{x' \in \mathcal{X}} \Delta^{\top}_{(S);x,x'} S_{x'},\\ \dot{I}_x = \beta_x S_x I_x - \gamma_x I_x - \mu_{(I)} \sum_{x' \in \mathcal{X}} \Delta^{\top}_{(I);x,x'} I_{x'},\\ \dot{R}_x = \gamma_x I_x - \mu_{(R)} \sum_{x' \in \mathcal{X}} \Delta^{\top}_{(R);x,x'} R_{x'},\end{cases}$$

for every $x \in \mathcal{X}$.

We define an invariant weighted mobility network D, representing the pre-epidemic traffic between subpopulations. Two subpopulations are considered neighbors if and only if the mobility network weight is non-zero. To ensure that the mobility network does not affect population sizes over time, it must be undirected, meaning the net flow of travelers between two subpopulations is equal in both directions. This condition is difficult to implement when subpopulations have heterogeneous size distributions. Our model resolves this issue by making the mobility rate between two subpopulations proportional to the product of their population sizes, resulting in equal diffusion in both directions. The base mobility rate between subpopulations is represented by a positive symmetric matrix W, and the mobility network is defined as:

$$D_{ij} = N_i N_j W_{ij}.$$

To incorporate adaptivity, subpopulations can restrict the mobility rate through a scalar travel restriction factor t. The travel restriction factor for a connection between two subpopulations ranges from zero to one, where one eliminates all mobility and zero allows full mobility. A value of zero, however, does not guarantee a pre-pandemic mobility rate, as the other side of the link could be implementing a travel restriction. Each subpopulation can control the level of travel restriction independently for each neighboring subpopulation, forming a vector $\mathbf{t}$ of travel restriction values. The values in the vector that would correspond to links to non-neighbors or the self-link equal zero. These vectors are combined to form a non-symmetric square matrix T, where $\Delta = T \circ T^{\top} \circ D$.

A more refined version of the equations for subpopulation i in vector form is:

$$\dot{S}_i = -\beta S_i I_i - \sum_{\substack{j=1 \\ j\neq i}}^{n} \mathbf{t}_i \mathbf{t}_j \mathbf{d}_j S_j,$$

$$\dot{I}_i = \beta S_i I_i - \gamma I_i - \sum_{\substack{j=1 \\ j\neq i}}^{n} \mathbf{t}_i \mathbf{t}_j \mathbf{d}_j I_j,$$

$$\dot{R}_i = \gamma I_i - \sum_{\substack{j=1 \\ j\neq i}}^{n} \mathbf{t}_i \mathbf{t}_j \mathbf{d}_j R_j.$$

A few deductions can be immediately made for this model formulation. First of all, it can be easily proven that the steady state of a subpopulation under SIR is either infection-free where the infection has not been introduced or has undergone infection and has fully recovered from it. Secondly, due to the nature of diffusion, it is to be expected that once a subpopulation contains a nonzero amount of infected individuals, it immediately spreads to not only all neighboring subpopulations, but all subpopulations in the connected component or subgraph of the infected subpopulation. The combination of these two observations is crucial as it eliminates the possibility of finding a travel restriction strategy that eradicates the disease in the metapopulation without all individuals getting infected once. There are several ways to counteract this issue, one which was explored is introducing the discrete probabilistic dynamics of interacting and migrating individuals, which does have a chance for an early end of the spread [**?**]. While it is true that preventing an epidemic from spreading to neighboring sites has been found to be very difficult, the instantaneous spread of the disease across all connected nodes is an unrealistic phenomenon. However, since the focus of this work is to slow down the spread of the infection and not completely eradicating it, this simplification is acceptable.

3 Strategies

To model the travel restrictions implemented as the prevalence of infection in the metapopulation changes over time, several strategies were explored. For each subpopulation x, given the control vector $\mathbf{t}$, it is desirable to minimize the mobility of infected individuals, I_x, down to zero. Since implementing travel restrictions typically takes a nonzero amount of time, giving a subpopulation the ability to immediately change the travel restriction to any desired value is unrealistic. The option of cutting off the connection to an infected population after a set time has been explored [**?**]. Instead, here the subpopulations have control over the rate of change of $\mathbf{t}$, which defines how $\mathbf{t}$ changes with time. Henceforth, a strategy defines an equation that $\dot{\mathbf{t}}$ follows given the current information about the metapopulation.

3.1 Global proportional travel restriction

The most basic form of travel restriction for the metapopulation is one where only the global infection prevalence is used to control restriction for all connections. This global travel restriction amounts to a single scalar value t that subpopulations implement, which scales down the mobility of all individuals across all subpopulation connections, from both origin and destination. This results in the equation:

$$\dot{t} = \lambda M_{(I)}$$

where $M_{(I)}$ is the total mobility of infected individuals on all connections:

$$M_{(I)} = \sum_{i=1}^{n} \sum_{j=1}^{i-1} \mathbf{t}_i \mathbf{t}_j \mathbf{d}_j I_j$$

Applying this global restriction on the metapopulation network, the final effective Laplacian of the network is:

$$\Delta_G = t^2 D$$

3.2 Uniform proportional travel restriction

A slightly more granular strategy would be for each subpopulation to look at the influx of infected individuals from all neighbors and restrict all connections uniformly based on the total number of infected individuals. This gives each subpopulation a single scalar variable t_x to control. This restriction follows the ODE:

$$\dot{t_x} = \lambda M_{(I);x}$$

where:

$$M_{(I);x} = \sum_{x' \in X}^{n} \mathbf{t}_x \mathbf{t}_{x'} \mathbf{d}_{x'} I_{x'}$$

3.3 Connection proportional travel restriction

Finally, a third strategy is investigated where subpopulations are given individual control over restrictions for each connection to neighbors. The strategy for a connection from subpopulation x to subpopulation x' is:

$$\dot{t}_{xx'} = \lambda M_{(I);x,x'}$$

where:

$$M_{(I);x,x'} = t_x t_{x'} d_{x'} I_{x'}$$

Unlike the other two strategies, this one is entirely local to the connection, and hence the resulting system can be classified under adaptive dynamical weighted networks[**?**].